



Published in final edited form as:

Kidney Int. 2015 June ; 87(6): 1164–1175. doi:10.1038/ki.2014.427.

Glycogen synthase kinase-3 β promotes cyst expansion in polycystic kidney disease

Shixin Tao^a, Vijayakumar Kakade^a, James Woodgett^b, Pankaj Pandey^a, Erin Suderman^a, Madhumitha Rajagopal^a, and Reena Rao^a

^aThe Kidney Institute, Department of Medicine, University of Kansas Medical Center, Kansas City, KS, USA. 66160

^bSamuel Lunenfeld Research Institute, Mount Sinai Hospital and Department of Medical Biophysics, University of Toronto, Ontario, Canada.

Abstract

Polycystic kidney diseases (PKDs) are inherited disorders characterized by the formation of fluid filled renal cysts. Elevated cAMP levels in PKDs stimulate progressive cyst enlargement involving cell proliferation and transepithelial fluid secretion often leading to end stage renal disease. The glycogen synthase kinase-3 (GSK3) family of protein kinases consists of GSK3 α and GSK3 β isoforms and plays a crucial role in multiple cellular signaling pathways. We previously found that GSK3 β , a regulator of cell proliferation, is also crucial for cAMP generation and vasopressin mediated urine concentration by the kidneys. However, the role of GSK3 β in the pathogenesis of PKDs is not known. Here we found that *GSK3 β* expression and activity were markedly up-regulated and associated with cyst-lining epithelia in the kidneys of mice and humans with PKD. Renal collecting duct specific gene knockout of *GSK3 β* or pharmacological inhibition of GSK3 effectively slowed the progression of PKD in mouse models of autosomal recessive or autosomal dominant PKD. GSK3 inactivation inhibited cAMP generation and cell proliferation resulting in reduced cyst expansion, improved renal function and extended lifespan. GSK3 β inhibition also reduced pERK, c-Myc and Cyclin-D1, known mitogens in proliferation of cystic epithelial cells. Thus, GSK3 β plays a novel functional role in PKD pathophysiology and its inhibition may be therapeutically useful to slow cyst expansion and progression of PKD.

Keywords

ADPKD; vasopressin; chronic kidney disease; cell signaling

Users may view, print, copy, and download text and data-mine the content in such documents, for the purposes of academic research, subject always to the full Conditions of use:http://www.nature.com/authors/editorial_policies/license.html#terms

Corresponding Author: Reena Rao The Kidney Institute, Dept. of Medicine, Univ. of Kansas Medical Center 3901 Rainbow Blvd, Kansas City KS 66160-3018, USA. 913 945 6885 - Phone 913 588 9251 - Fax rrao@kumc.edu.

Disclosures: The authors declare that no conflict of interest exists.

INTRODUCTION

Progressive cyst enlargement in PKD is associated with abnormal cell proliferation, loss of cell differentiation and polarity, and increased luminal fluid secretion that obliterates the renal architecture, often leading to renal failure ¹. Understanding the molecular basis of PKD is important for the identification of targets for diagnosis and treatment of this disease. Cyclic AMP, a ubiquitous and versatile second messenger is elevated in PKD and stimulates proliferation and fluid secretion by the cyst lining epithelial cells ²⁻⁸. In a normal kidney, extracellular ligand binding leads to G protein-coupled receptor (GPCR)-mediated activation of adenylate cyclase, and thereby cAMP generation. In PKD, renal cAMP levels are elevated due to a) activation of calcium-inhibitable adenylate cyclase and inhibition of calcium-activated phosphodiesterases, b) loss of polycystin-1 mediated suppression of adenylate cyclase activity and c) enhanced vasopressin (AVP) signaling through its type-2 receptor (V2R) which activates adenylate cyclase ⁵. The importance of cAMP in PKD is further supported by studies in which reducing cAMP levels by inhibition of V2R or lack of AVP reduces cystogenesis in rodent models of PKD ^{9, 10}.

The GSK3 α and GSK3 β isoforms regulate multiple fundamental cellular processes by modulating cell-signaling pathways and are targets for drug development in cancer, Alzheimer's disease and diabetes ^{11, 12}. In certain forms of cancer, GSK3 plays a tumor promoter role mainly by increasing cell proliferation ¹³, but its role in renal cyst expansion in PKD has not been examined. Importantly in the kidney, GSK3 β is crucial for AVP sensitive adenylate cyclase activity and cAMP generation. Lithium, a common treatment for bipolar disorders has been for long thought to inhibit adenylate cyclase activity and reduce cAMP ¹⁴⁻¹⁷, though it had no effect on cAMP levels in dDAVP treated Brattleboro rats ¹⁸. Lithium is also a non-specific inhibitor of GSK3. In previous studies we demonstrated that pharmacological inhibition using a highly specific GSK3 inhibitor or renal collecting duct specific knockout of GSK3 β can significantly reduce adenylate cyclase activity and cAMP accumulation ¹⁹. Hence we hypothesized that inactivation of GSK3 could reduce renal cAMP levels and cyst expansion in PKD.

To test the pathophysiological role of GSK3 in renal cyst development in PKD, we used the *Cys1^{cpk}* mouse, a well-characterized mouse model of autosomal recessive polycystic kidney disease (ARPKD) that carries a gene mutation for *Cys1*. Though non-orthologous, this mouse model closely mimics human ARPKD ²⁰⁻²². Postnatal renal cyst enlargement in *Cys1^{cpk}* mice is rapid, resulting in death at approximately 3 weeks of age. Importantly, *Cys1^{cpk}* mice are known to exhibit increased vasopressin receptor expression, proto-oncogenes and cell proliferation ^{20, 23, 24}. We also used the *PKD1^{fl/fl}:PKHD1^{cre}* mouse, an orthologous model for autosomal dominant polycystic kidney disease (ADPKD) which is also characterized by increased renal cell proliferation ²⁵⁻²⁷. Systemic GSK3 inhibition or collecting duct specific *GSK3 β* gene deletion was carried out in these mouse models of PKD were employed to analyze mechanism. The results of these studies are presented.

RESULTS

Abnormal renal GSK3 expression in PKD

To determine the role of GSK3 in PKD, we examined GSK3 α and GSK3 β expression in cystic mouse and human kidneys. In *Cys1^{cpk}* mice, cysts develop during late embryogenesis and expand rapidly resulting in death around postnatal day-21 (P21) while in *PKDI^{ff}:PKHDI^{cre}* mice, renal cysts appear by P12-P14 and death occurs by P40. Renal GSK3 β protein levels were significantly high in *Cys1^{cpk}* mice by P14 and in *PKDI^{ff}:PKHDI^{cre}* mice by P21, compared to their wild type mice (WT) littermates (Fig-1a). Unlike GSK3 β , GSK3 α and pGSK3 α levels showed no significant change in both PKD models compared to WT mice (Fig-1a). Renal GSK3 β protein levels in *Cys1^{cpk}* mice were unchanged at P7 (data not shown). GSK3 β activity was also increased in *Cys1^{cpk}* and *PKDI^{ff}:PKHDI^{cre}* mice, indicated by the reduced inactive pGSK3 β (phospho-GSK3 β -serine 9) to total GSK3 β ratio (Fig-1a,b,c). Similarly in human ADPKD kidneys, immunostaining for pGSK3 β was low or absent in cyst lining epithelia in spite of high GSK3 β expression in cyst lining epithelium (Fig-1d). In *Cys1^{cpk}* mice, *GSK3 β* mRNA levels were significantly higher while *GSK3 α* mRNA levels were unchanged compared to WT mice (Fig-1e). In *PKDI^{ff}:PKHDI^{cre}* mouse and human ADPKD kidneys, mRNA levels of *GSK3 β* and to a lesser extent, *GSK3 α* were increased compared to WT mouse or control human kidneys respectively (Fig-1f, g). Since GSK3 isoforms are known to be regulated at the level of their activity rather than total protein²⁸, this aberrant renal GSK3 expression in PKD is a novel finding in renal pathophysiology.

In *Cys1^{cpk}* mice, renal cysts at P0 were mostly of proximal tubule origin (identified by *Lotus tetragonolobus* agglutinin, green staining), while the enlarged cysts at P7 and P14 were of collecting duct origin (identified by *Dolichos biflorous*, red staining) (Fig-2a). At P14, intense staining for GSK3 β was observed in the cyst-lining cells in *Cys1^{cpk}* mice, while GSK3 α expression was restricted mostly to smaller cysts or non-cystic tubules (Fig-2b). In WT littermates, ubiquitous staining for GSK3 α and GSK3 β was observed in renal tubules (Fig-2b). GSK3 β staining was observed in all cyst lining epithelia in *Cys1^{cpk}*, *PKDI^{ff}:PKHDI^{cre}* and human ADPKD kidneys and most of the enlarged cysts were of collecting duct origin and not proximal tubular (Fig-2c,d). The location of GSK3 β in cyst-lining epithelium and its higher expression levels in cystic kidneys of both ADPKD and ARPKD mouse models as well as humans suggest that GSK3 β could be mechanistically involved in abnormal cell signaling and cyst enlargement in PKD.

Systemic GSK3 inhibition reduced cysts and preserved renal function in PKD

To determine the pathophysiological role of GSK3 in PKD, we tested the effect of pharmacological inhibition of GSK3 on cyst development in *Cys1^{cpk}* and *PKDI^{ff}:PKHDI^{cre}* mice. TDZD-8^{29,30}, is a highly selective, ATP non-competitive inhibitor of GSK3 that others and we have effectively used in mice^{29,31}. TDZD-8 was administered to *Cys1^{cpk}* and WT littermates from P3 until P14 and to *PKDI^{ff}:PKHDI^{cre}* and WT littermates from P10 until P21. TDZD-8 treatment in both *Cys1^{cpk}* and *PKDI^{ff}:PKHDI^{cre}* mice significantly reduced overall kidney size and preserved more intact parenchyma (Fig-3a). TDZD-8 treatment also reduced renal cyst area and cyst number in

Cys1^{cpk} mice (Fig-3b,c) as well as in *PKD1^{ff}:PKHD1^{cre}* mice (Fig-3d,e) compared to vehicle treatment.

TDZD-8 treatment reduced kidney to body weight ratio by 37% and blood urea nitrogen (BUN) levels by 36% (Fig-3f,g) in *Cys1^{cpk}* mice. Similarly in *PKD1^{ff}:PKHD1^{cre}* mice, TDZD-8 treatment reduced kidney to body weight ratio by 28% (Fig-3h) and BUN by 37% (Fig-3i), compared to vehicle treatment. TDZD-8 treated *Cys1^{cpk}* and WT mice did not show a significant difference in body weight (Supplemental-1). These results suggest that GSK3 inhibition could reduce cyst development and expansion in *Cys1^{cpk}* and *PKD1^{ff}:PKHD1^{cre}* mice.

Collecting duct specific gene knockout of *GSK3 β* slowed PKD and increased life span

To evaluate further the isoform-selective and tissue specific role of GSK3 β on cyst expansion, we generated *Cys1^{cpk}* and *PKD1^{ff}:PKHD1^{cre}* mice lacking *GSK3 β* in renal collecting ducts (*Cys1^{cpk}+GSK3 β ^{CD-KO}* and *PKD1^{ff}:GSK3:PKHD1^{cre}*). Collecting duct specific gene deletion of *GSK3 β* was achieved using *HoxB7^{cre}* in *Cys1^{cpk}+GSK3 β ^{CD-KO}* mice and *PKHD1^{cre}* in *PKD1^{ff}:GSK3:PKHD1^{cre}* mice. Immunostaining of kidney sections showed no staining for GSK3 β in collecting duct cysts of *Cys1^{cpk}+GSK3 β ^{CD-KO}* and *PKD1^{ff}:GSK3:PKHD1^{cre}* mice (Fig-4a), while GSK3 β staining was observed in other tubule segments (Supplemental-2). Proximal tubular cysts were observed in *Cys1^{cpk}+GSK3 β ^{CD-KO}* and not *PKD1^{ff}:GSK3:PKHD1^{cre}* mice (Supplemental-2). In comparison to *Cys1^{cpk}* kidneys, the *Cys1^{cpk}+GSK3 β ^{CD-KO}* kidneys had more intact parenchyma and were less cystic (Fig-4b). The kidney to body weight ratio and BUN levels were also lower in *Cys1^{cpk}+GSK3 β ^{CD-KO}* mice compared to *Cys1^{cpk}* mice (Fig-4c,d). Similarly in *PKD1^{ff}:PKHD1^{cre}* mice, collecting duct specific gene knockout of *GSK3 β* also significantly reduced overall kidney size (Fig-4b), kidney to body weight ratio and BUN (Fig-4e,f). Consistent with their slower cyst progression, the life span of the *Cys1^{cpk}+GSK3 β ^{CD-KO}* mice increased by 25% compared to *Cys1^{cpk}* mice (Fig-4g). This suggests that GSK3 β in collecting ducts play an important role in cyst development in the *Cys1^{cpk}* and *PKD1^{ff}:PKHD1^{cre}* mice.

GSK3 inhibition reduced proliferation of cyst lining epithelial cells

In order to examine the mechanism by which GSK3 regulates renal cyst expansion, we determined the effect of GSK3 β inhibition on cell proliferation, a central contributor to cyst enlargement in PKD, and a cellular process regulated by GSK3. In vehicle treated *Cys1^{cpk}* and *PKD1^{ff}:PKHD1^{cre}* mice, immunostaining for KI-67 and PCNA revealed a large number of dividing cells (Fig-5a,b). TDZD-8 treatment significantly reduced the number of dividing cells in both *Cys1^{cpk}* and *PKD1^{ff}:PKHD1^{cre}* mouse kidneys (Fig-5a,b,c,d).

A variety of pro-proliferative transcription factors/co-activators and cell cycle regulators such as β -catenin, c-Myc and Cyclin-D1 are important for cyst enlargement in PKD^{23, 32-35}. c-Myc and Cyclin-D1 levels were significantly increased in *Cys1^{cpk}* mice when compared to WT mice (Fig-5 e,f,g, Supplemental-3). Beta-catenin level on the other hand was significantly reduced in *Cys1^{cpk}* kidneys compared to WT kidney and β -catenin immunostaining was not associated with cystic epithelium (Fig-5c, Supplemental-3). The

protein and mRNA levels of β -catenin was also found to be reduced by 40-50% in the *Cys1^{cpk}* and *PKD1^{ff}:PKHD1^{cre}* mice respectively (Supplemental-4,5,6,7), suggesting that β -catenin may not be critical for proliferation of the cyst lining epithelium in these mice. TDZD-8 treatment reduced Cyclin-D1 and (Fig-5e,f, Supplemental-8) c-Myc (Fig-5e,g) levels in *Cys1^{cpk}* mice, while β -catenin levels increased (Fig-5e). The reduced c-Myc and Cyclin-D1 levels in *Cys1^{cpk}* mice support the reduced cell proliferation indicated by PCNA staining observed in these mice. Thus, GSK3 inhibition could reduce proliferation of cyst lining epithelial cells and thereby cyst expansion.

GSK3 inhibition reduced renal cAMP and activation of ERK1/2

Since cAMP stimulates proliferation of cyst-lining epithelial cells³⁶, we determined the effect of GSK3 inhibition on renal cAMP. In *Cys1^{cpk}* and *PKD1^{ff}:PKHD1^{cre}* mice, renal cAMP levels were 7 and 6-folds higher compared to their respective WT littermates. TDZD-8 treatment reduced renal cAMP by 33% in *Cys1^{cpk}* mice and 39% in *PKD1^{ff}:PKHD1^{cre}* mice when compared to their vehicle treated controls (Fig-6a,b).

Cyclic AMP mediated activation of B-Raf/ERK/MAPK pathway is known to increase cell proliferation in cultured PKD cells³⁷ and regulate c-Myc and Cyclin-D1 expression levels³⁸. In *Cys1^{cpk}* and *PKD1^{ff}:PKHD1^{cre}* mouse kidneys, the pERK levels were significantly higher than in WT littermates (Fig-6c,d,e,f). Treatment with TDZD-8 significantly reduced pERK/ERK ratio in both models (Fig-6c,d,e,f). The reduced cAMP and ERK activation in the TDZD-8 treated PKD mice are consistent with their reduced c-Myc and Cyclin-D1 levels and support the reduced cell proliferation indicated by PCNA staining observed in these mice. Thus, GSK3 is important for cAMP-mediated proliferation by cyst lining epithelial cells in PKD and its inactivation can slow cAMP induced cyst expansion in mouse models of PKD.

DISCUSSION

The current studies demonstrate a novel functional role of GSK3 β in renal cyst development and progression of PKD. Our conclusions are based on the key observations that, 1) GSK3 β expression is increased and associated with cyst lining epithelium in ARPKD and ADPKD mouse models and human ADPKD kidney, and 2) pharmacological inhibition or collecting duct specific gene deletion of *GSK3 β* protects renal structure and function and slows cyst expansion in *Cys1^{cpk}* and *PKD1^{ff}:PKHD1^{cre}* mice. Examination of mechanism demonstrated that GSK3 β inactivation was associated with reduced intracellular cAMP generation and cell proliferation. GSK3 inhibition suppressed ERK pathway activation, and reduced c-Myc and Cyclin-D1 levels, resulting in reduced cell proliferation. Overall, these studies revealed a previously undescribed role of GSK3 in the pathogenesis of cyst expansion.

GSK3 is an important regulatory component of fundamental processes including epithelial cell differentiation, polarity and proliferation³⁹. It is known to be ubiquitously expressed and constitutively active in the absence of external stimuli^{11, 12}. Since WNT and growth factor mediated signaling which inhibit GSK3¹² are active in PKD^{32, 40}, it could be assumed that GSK3 β activity is suppressed in PKD. On the contrary, the current studies not

only found an increase in GSK3 β activity in cystic kidneys, but also a significant increase in its expression. It is also significant that GSK3 β expression was found to be especially high in collecting ducts, which respond to AVP, undergo proliferation, secrete fluid and are the primary source of cysts in PKD^{9,41,42}. Thus GSK3 β could have a pathological role in renal cyst expansion.

Evidence implicating GSK3 β in the pathogenesis of PKD was provided by our studies in which treatment with a highly specific inhibitor of GSK3 or collecting duct specific gene deletion of GSK3 β slowed the progression of cyst expansion. This observation can be said to be unexpected, because lithium treatment is thought to be associated with renal cyst development. Renal cysts have been observed in patients on long-term lithium therapy with known or unknown familial history of PKD⁴³⁻⁴⁵. Similarly, postnatal exposure to LiCl through mother's milk produced renal collecting duct microcysts in male rats⁴⁶, although adult rats treated with LiCl for over 40 days showed increased cell proliferation but no cysts^{47,48}. Hence it is not clear if inhibition of GSK3, one among the many activities of lithium, is the mechanism for cyst formation. Moreover, the renal collecting duct specific GSK3 β knockout mice used in the current studies and described earlier¹⁹ do not show any renal cysts for up to two years of age. In the current study, the reduction in kidney weight / body weight ratio in TDZD-8 treated *Cys1^{cpk}* mice (37%) and *PKD1^{ff}:PKHDI^{cre}* mice (28%) are comparable to other recent preclinical studies using PP242 (mTOR kinase inhibitor)⁴⁹, R-roscovitin (Cyclin Dependent Kinase inhibitor)⁵⁰, STA-2842 (Heat shock protein 90 inhibitor)⁵¹, Tolvaptan+Rapamycin⁵² or Tolvaptan+Pasireotide⁵³, to name a few.

Inhibition or gene deletion of GSK3 slowed the progression of cyst expansion by reducing proliferation of cyst lining epithelial cells. Proliferation of the cystic epithelium is critical for the development and enlargement of renal cysts^{25,54,55} and progressive cyst enlargement in both ADPKD and ARPDK involve increased proliferation of cyst-lining epithelial cells³⁶. Hence various growth factors and their receptors, oncogenes and cell cycle regulatory proteins that regulate cell proliferation have been studied as possible targets for the treatment of PKD⁵⁶. β -catenin, a crucial component of canonical WNT-signaling is thought to be important in PKD^{35,57}, although no increase in β -catenin/TCF/Lef1 activity has been detected in renal cyst lining epithelial cells^{35,58-61}. In the current study, β -catenin was significantly reduced in both *Cys1^{cpk}* and *PKD1^{ff}:PKHDI^{cre}* mice, compared to wild type mice (Supplemental data 3-7). β -catenin is a substrate of GSK3 β , which negatively regulates its cytoplasmic accumulation³⁹. Hence the decreased β -catenin level in *Cys1^{cpk}* mice is consistent with their increased GSK3 β activity and increased β -catenin after TDZD-8 treatment corresponds to the reduced GSK3 β activity. Alternately, it is also possible that β -catenin expression is independent of GSK3 β in the PKD kidney, because in GSK3 β global knock out mice, β -catenin levels did not increase⁶². Similarly in colon cancer, both β -catenin as well as GSK3 β are up regulated and involved in pathogenesis⁶³.

Regulation of cell proliferation is a basic function of GSK3, although its role is context dependent. GSK3 inhibition enhances proliferation of embryonic and hematopoietic stem cells^{64,65}, embryonic cardiomyocytes⁶⁶, cancer cells¹³ and accelerates regeneration of proximal tubular cells following acute kidney injury²⁹. However, GSK3 inhibition can also

reduce cell proliferation and tumor progression in ovarian, myeloma, leukemia, pancreatic, colorectal and hepatic cancers by inducing cell cycle arrest and reducing mitogenic factors ⁶⁷⁻⁷².

Our results demonstrate that GSK3 could regulate cell proliferation in PKD by a cAMP-dependent mechanism. GSK3 inhibition by TDZD-8 reduced cAMP levels in both *Cys1^{cpk}* and *PKD1^{ff}:PKHD1^{cre}* mouse models. Cyclic AMP mediated activation of B-Raf/ERK pathway increases cell proliferation in cultured PKD cells ³⁷. In-vivo, activation of the B-Raf/ERK pathway has been observed in rodent models of PKD, but its role in proliferation of cyst lining epithelial cells has been inconclusive ^{26, 73}. ERK/MAPK activity can induce expression of c-Myc and Cyclin-D1 ³⁸, which are important factors for proliferation in PKD ^{23, 32-35}. In the current studies, renal ERK activity, Cyclin D1 and c-Myc levels were high in the *Cys1^{cpk}* mice and TDZD-8 treatment significantly reduced their levels. C-Myc and Cyclin-D1 are primary molecular targets of GSK3 β for phosphorylation-dependent protein degradation in the ubiquitin–proteasome system ³⁹. However, in normal WT mice, TDZD-8 treatment did not increase C-Myc and Cyclin-D1 levels (fig-5). Hence, the reduced c-Myc and Cyclin-D1 levels in *Cys1^{cpk}*+TDZD-8 mice are more consistent with observations in cancer cells in which inhibition of GSK3 can reduce c-Myc and Cyclin-D1 levels and suppress cell proliferation ^{68, 70, 71}.

In summary, renal GSK3 β expression is up-regulated in PKD and plays an important role in cAMP-mediated proliferation and anion secretion by cyst lining epithelial cells. Pharmacological inhibition of GSK3 or collecting duct specific gene deletion of GSK3 β reduced cyst volume and delayed cyst progression. The results thus demonstrate a novel pathological role of GSK3 β in promoting renal cyst expansion. Use of a GSK3 inhibitor may be therapeutically useful to reduce cyst expansion and preserve renal function in PKD.

METHODS

Mouse Studies

The *Cys1^{cpk/+}* mice were originally purchased from the Jackson Laboratory (Bar Harbor, ME). Mouse pups were genotyped on postnatal day 2 (P2). For TDZD-8 treatment, WT and *Cys1^{cpk}* mouse littermates were treated with TDZD-8 (5mg/kg body weight) or vehicle (5% DMSO in saline) from P3 until P14 by single, daily, intra-peritoneal injections. This dose of TDZD-8 was selected based on results from our pilot study and was found to be better than a dose of 1mg/Kg bodyweight in reducing kidney to bodyweight ratio in *Cys1^{cpk}* mice. Similarly, *PKD1^{ff}:PKHD1^{cre}* ²⁶ mice were injected with TDZD-8 from P10 until P21.

To generate *Cys1^{cpk}* mice lacking GSK3 β in renal collecting ducts, the *Cys1^{cpk}* mice were bred with *GSK3 β ^{ff}:HoxB7^{cre}* mice ¹⁹. Mouse pups of the following genotypes-*GSK3 β ^{ff}* (WT), *Cys1^{cpk}*+*GSK3 β ^{ff}:HoxB7^{cre}* (*Cys1^{cpk}*+*GSK3 β ^{CD-KO}*), and *Cys1^{cpk}* were mice were used for the studies. Similarly, *PKD1^{ff}:PKHD1^{cre}* mice were bred with *GSK3 β ^{ff}* mice to generate *PKD1^{ff}:PKHD1^{cre}* mice lacking GSK3 β in the collecting duct. *PKD1^{ff}* (WT), *PKD1^{ff}:GSK3 β ^{ff}:PKHD1^{cre}* and *PKD1^{ff}:PKHD1^{cre}* mice were used for the studies. Body weight was measured daily. At sacrifice, blood and urine samples were collected, and kidneys were weighed and flash frozen for protein and RNA analysis or fixed in 4%

paraformaldehyde for histological examination. All mouse study protocols were approved by the University of Kansas Medical Center Institutional Animal Care and Use Committee.

Quantification of Cysts and Cell Proliferation—The kidney (left and right kidneys) / body weight % and cyst area were used as indicators of cyst progression. Cyst surface area was measured from 10 random fields (x100 magnification) from hematoxylin and eosin stained tissue sections (5 μ Lm) of paraffin-embedded kidneys. Images were obtained with a dissection microscope connected to a digital camera (Leica Microsystems, Buffalo Grove, IL). A blinded observer determined cyst number and cystic cross-sectional SA per kidney section using LUZEX FS software (Kideko CO. LTD, Tokyo, Japan).

For quantification of cell proliferation, tissue sections were immunostained for KI-67 and PCNA, and the cells stained for KI-67 or PCNA and total number of cells in each cyst-lining epithelium were counted from 10 random fields (x200 magnification). A reviewer, blinded to the identity of the mouse kidney, performed measurements.

Blood Urea Nitrogen (BUN) Levels—Blood was collected at sacrifice and immediately centrifuged at 2,000xg for serum collection. BUN levels were measured using a QuantiChrom Urea Assay Kit from BioAssay Systems (Hayward, CA, USA).

Western Blot—Mouse kidneys were homogenized in RIPA buffer and loaded onto 12% SDS-PAGE gels and transferred to nitrocellulose membranes and blocked with 5% milk in TBST. Membranes were probed with primary antibody followed by TBST washes and horseradish peroxidase secondary antibody application. The following antibodies were used, GSK3 α , GSK3 β , pGSK3 α , pGSK3 β , β -Catenin, Cyclin-D1 (Cell Signaling Technology, Inc., MA, USA), c-Myc, GAPDH, pERK and ERK (Santa Cruz Biotechnology, Inc. TX, USA). Secondary antibodies were purchased from Dako (CA, USA) and ECL reagent from PerkinElmer (Netherlands).

Immunohistochemistry/Immunofluorescence (IHC/IF)—Fixed kidney tissues were embedded in paraffin. For both IHC and IF, sections were deparaffinized, rehydrated, washed in PBS containing 0.1% Tween 20 (PBST) and blocked in 10% normal goat serum. The following primary antibodies were applied to sections and incubated at 4 $^{\circ}$ C overnight: β -Catenin, cyclin D1, KI-67 and pGSK3 β (Cell Signaling Technology, Inc., MA, USA), GSK α (Sigma Aldrich, MO, USA), GSK3 β (Santa Cruz Biotechnology, Inc. TX, USA), PCNA (Dako, CA, USA), DBA and LTA (Vector Laboratories, CA, USA). For IHC, slides were blocked with Avidin/Biotin (Invitrogen), and then biotinylated goat anti-rabbit IgG or anti-mouse IgG (Invitrogen, NY, USA) secondary antibodies were applied, followed by incubation with Streptavidin HRP conjugate (Invitrogen, NY, USA). Finally slides were developed with DAB (Vector Laboratories) and counterstained with Harris Haematoxylin, dehydrated, and mounted with Permount (Fisher Scientific). For IF, after incubation with primary antibody, goat anti-Rabbit IgG fluor, Goat anti-mouse IgG Texas red (Invitrogen, NY, USA), or Goat anti-chicken IgG Alexa 555 (Sigma Aldrich, MO, USA) secondary antibodies were applied, and following incubation, washed, stained with DAPI and mounted with Flour-G (Invitrogen, NY, USA). All images were captured using a Nikon 80i microscope in KUMC imaging center.

Quantitative Real-Time PCR

Quantitative real-time PCR on RNA isolated from whole kidney samples were carried out as described before¹⁹. The *18S*, *GSK3 α* and *GSK3 β* probes were obtained from Applied Biosystems, Foster City, CA, USA.

Measurement of cAMP—A cAMP Enzyme Immunoassay Kit (Direct) from Sigma-Aldrich (MO,USA) was used. The kidneys were ground to a fine powder under liquid nitrogen and homogenized in 10 volumes of ice cold 0.1% HCl, centrifuged at 600xg and cAMP levels measured following the manufacturer's protocols.

Human Tissue—Human control and ADPKD kidney tissues were obtained from the National disease research interchange and were approved by the institutional review board.

Statistics—Values are expressed as mean \pm standard error for all bar charts, except for band density measurements of western blots, which is expressed as mean \pm standard deviation. Data was analyzed by two-tailed unpaired t-test with Welch's correction and F test to compare variances or One-Way Analysis of Variance followed by Tukey's multiple comparison test and Bartlett's test for equal variance using Graphpad Prism software (Version 5.0d). A probability level of 0.05 ($P < 0.05$) was considered significant. To compare survival curves, Log-rank (Mantel-cox) Test and Gehan-Breslow-Wilcoxon Test were used.

Supplementary Material

Refer to Web version on PubMed Central for supplementary material.

ACKNOWLEDGEMENTS

We thank Drs. Alan Yu, James Calvet, Robin Masser and Jared Grantham for helpful discussions, Dr. Peter Igarashi for *PKHD1^{CRE}* mice, Dr. Stefan Somlo and the Yale PKD Center (P30 DK090744) for *PKD1^{f/f}* mice. This study was supported by NIH R01-DK083525 to Rao.

REFERENCES

1. Grantham JJ, Mulamalla S, Swenson-Fields KI. Why kidneys fail in autosomal dominant polycystic kidney disease. *Nat Rev Nephrol.* 2011; 7:556–566. [PubMed: 21862990]
2. Choi YH, Suzuki A, Hajarnis S, et al. Polycystin-2 and phosphodiesterase 4C are components of a ciliary A-kinase anchoring protein complex that is disrupted in cystic kidney diseases. *Proc Natl Acad Sci.* 2011; 108:10679–10684. [PubMed: 21670265]
3. Fonseca JM, Bastos AP, Amaral AG, et al. Renal cyst growth is the main determinant for hypertension and concentrating deficit in *Pkd1*-deficient mice. *Kidney Intl.* 2014; 85:1137–1150.
4. Gattone VH 2nd, Wang X, Harris PC, et al. Inhibition of renal cystic disease development and progression by a vasopressin V2 receptor antagonist. *Nat Med.* 2003; 9:1323–1326. [PubMed: 14502283]
5. Torres VE. Cyclic AMP, at the hub of the cystic cycle. *Kidney Intl.* 2004; 66:1283–1285.
6. Torres VE, Harris PC. Autosomal dominant polycystic kidney disease: the last 3 years. *Kidney Intl.* 2009; 76:149–168.
7. Wallace DP. Cyclic AMP-mediated cyst expansion. *Biochim Biophys Acta.* 2011; 1812:1291–1300. [PubMed: 21118718]

8. Yamaguchi T, Nagao S, Kasahara M, et al. Renal accumulation and excretion of cyclic adenosine monophosphate in a murine model of slowly progressive polycystic kidney disease. *Am J Kidney Dis.* 1997; 30:703–709. [PubMed: 9370187]
9. Torres VE, Wang X, Qian Q, et al. Effective treatment of an orthologous model of autosomal dominant polycystic kidney disease. *Nat Med.* 2004; 10:363–364. [PubMed: 14991049]
10. Wang X, Wu Y, Ward CJ, et al. Vasopressin directly regulates cyst growth in polycystic kidney disease. *J Am Soc Nephrol.* 2008; 19:102–108. [PubMed: 18032793]
11. Harwood AJ. Regulation of GSK-3: a cellular multiprocessor. *Cell.* 2001; 105:821–824. [PubMed: 11439177]
12. Kaidanovich-Beilin O, Woodgett JR. GSK-3: Functional Insights from cell biology and animal models. *Front Mol Neurosci.* 2011; 4:40. [PubMed: 22110425]
13. Mishra R. Glycogen synthase kinase 3 beta: can it be a target for oral cancer. *Mol Cancer.* 2010; 9:144. [PubMed: 20537194]
14. Goldberg H, Clayman P, Skorecki K. Mechanism of Li inhibition of vasopressin-sensitive adenylate cyclase in cultured renal epithelial cells. *Am J Physiol.* 1988; 255:F995–1002. [PubMed: 2461098]
15. Jackson BA, Edwards RM, Dousa TP. Lithium-induced polyuria: effect of lithium on adenylate cyclase and adenosine 3',5'-monophosphate phosphodiesterase in medullary ascending limb of Henle's loop and in medullary collecting tubules. *Endocrinol.* 1980; 107:1693–1698.
16. Mann L, Heldman E, Shaltiel G, et al. Lithium preferentially inhibits adenylyl cyclase V and VII isoforms. *Int J Neuropsychopharmacol.* 2008; 11:533–539. [PubMed: 18205980]
17. Yamaki M, Kusano E, Tetsuka T, et al. Cellular mechanism of lithium-induced nephrogenic diabetes insipidus in rats. *Am J Physiol.* 1991; 261:F505–511. [PubMed: 1716061]
18. Li Y, Shaw S, Kamsteeg EJ, et al. Development of lithium-induced nephrogenic diabetes insipidus is dissociated from adenylyl cyclase activity. *JASN.* 2006; 17:1063–1072. [PubMed: 16495377]
19. Rao R, Patel S, Hao C, et al. GSK3beta mediates renal response to vasopressin by modulating adenylate cyclase activity. *J Am Soc Nephrol.* 2010; 21:428–437. [PubMed: 20056751]
20. Alcalay NI, Sharma M, Vassmer D, et al. Acceleration of polycystic kidney disease progression in cpk mice carrying a deletion in the homeodomain protein Cux1. *Am J Physiol Renal Physiol.* 2008; 295:F1725–1734. [PubMed: 18829740]
21. Gattone VH 2nd, MacNaughton KA, Kraybill AL. Murine autosomal recessive polycystic kidney disease with multiorgan involvement induced by the cpk gene. *Anat Rec.* 1996; 245:488–499. [PubMed: 8800407]
22. Hou X, Mrug M, Yoder BK, et al. Cystin, a novel cilia-associated protein, is disrupted in the cpk mouse model of polycystic kidney disease. *J Clin Invest.* 2002; 109:533–540. [PubMed: 11854326]
23. Cowley BD Jr, Chadwick LJ, Grantham JJ, et al. Elevated proto-oncogene expression in polycystic kidneys of the C57BL/6J (cpk) mouse. *J Am Soc Nephrol.* 1991; 1:1048–1053. [PubMed: 1912403]
24. Gattone VH 2nd, Maser RL, Tian C, et al. Developmental expression of urine concentration-associated genes and their altered expression in murine infantile-type polycystic kidney disease. *Dev Genet.* 1999; 24:309–318. [PubMed: 10322639]
25. Karihaloo A, Koraihy F, Huen SC, et al. Macrophages promote cyst growth in polycystic kidney disease. *J Am Soc Nephrol.* 2011; 22:1809–1814. [PubMed: 21921140]
26. Shibasaki S, Yu Z, Nishio S, et al. Cyst formation and activation of the extracellular regulated kinase pathway after kidney specific inactivation of Pkd1. *Hum Mol Genet.* 2008; 17:1505–1516. [PubMed: 18263604]
27. Zhou X, Fan LX, Sweeney WE Jr, et al. Sirtuin 1 inhibition delays cyst formation in autosomal-dominant polycystic kidney disease. *J Clin Invest.* 2013; 123:3084–3098. [PubMed: 23778143]
28. Medina M, Wandosell F. Deconstructing GSK-3: The fine regulation of its activity. *Int J Alzheimers Dis.* 2011; 2011:479249. [PubMed: 21629747]
29. Howard C, Tao S, Yang HC, et al. Specific deletion of glycogen synthase kinase-3beta in the renal proximal tubule protects against acute nephrotoxic injury in mice. *Kidney Intl.* 2012; 82:1000–1009.

30. Martinez A, Alonso M, Castro A, et al. First non-ATP competitive glycogen synthase kinase 3 beta (GSK-3beta) inhibitors: thiadiazolidinones (TDZD) as potential drugs for the treatment of Alzheimer's disease. *J Med Chem.* 2002; 45:1292–1299. [PubMed: 11881998]
31. Beurel E, Kaidanovich-Beilin O, Yeh WI, et al. Regulation of Th1 cells and experimental autoimmune encephalomyelitis by glycogen synthase kinase-3. *J Immunol.* 2013; 190:5000–5011. [PubMed: 23606540]
32. Gallagher AR, Germino GG, Somlo S. Molecular advances in autosomal dominant polycystic kidney disease. *Adv Chronic Kidney Dis.* 2010; 17:118–130. [PubMed: 20219615]
33. Ricker JL, Mata JE, Iversen PL, et al. c-myc antisense oligonucleotide treatment ameliorates murine ARPKD. *Kidney intl.* 2002; 61:S125–131.
34. Schwensen KG, Burgess JS, Graf NS, et al. Early cyst growth is associated with the increased nuclear expression of cyclin D1/Rb protein in an autosomal-recessive polycystic kidney disease rat model. *Nephron Exp Nephrol.* 2011; 117:e93–103. [PubMed: 20924203]
35. Wuebben A, Schmidt-Ott KM. WNT/beta-catenin signaling in polycystic kidney disease. *Kidney intl.* 2011; 80:135–138.
36. Grantham JJ. Regulation of cell proliferation and fluid secretion in the progressive enlargement of renal cysts. *Contrib Nephrol.* 1992; 97:15–22. [PubMed: 1633714]
37. Yamaguchi T, Wallace DP, Magenheimer BS, et al. Calcium restriction allows cAMP activation of the B-Raf/ERK pathway, switching cells to a cAMP-dependent growth-stimulated phenotype. *J Biol Chem.* 2004; 279:40419–40430. [PubMed: 15263001]
38. Chang F, Steelman LS, Shelton JG, et al. Regulation of cell cycle progression and apoptosis by the Ras/Raf/MEK/ERK pathway (Review). *Int J Oncol.* 2003; 22:469–480. [PubMed: 12579299]
39. Woodgett JR, Force T. Unique and overlapping functions of GSK-3 isoforms in cellular differentiation, proliferation, and cardiovascular development. *J Biol Chem.* 2008; 15:9643–7. [PubMed: 19064989]
40. Torres VE, Harris PC. Mechanisms of Disease: autosomal dominant and recessive polycystic kidney diseases. *Nat Clin Pract Nephrol.* 2006; 2:40–55. quiz 55. [PubMed: 16932388]
41. Verani RR, Silva FG. Histogenesis of the renal cysts in adult (autosomal dominant) polycystic kidney disease: a histochemical study. *Mod Pathol.* 1988; 1:457–463. [PubMed: 3065782]
42. Wu G, D'Agati V, Cai Y, et al. Somatic inactivation of Pkd2 results in polycystic kidney disease. *Cell.* 1998; 93:177–188. [PubMed: 9568711]
43. Atagun MI, Oral ET, Sevinc C. [Polycystic kidney disease in a patient using lithium chronically]. *Turk Psikiyatri Derg.* 2013; 24:213–216. [PubMed: 24049011]
44. Farres MT, Ronco P, Saadoun D, et al. Chronic lithium nephropathy: MR imaging for diagnosis. *Radiology.* 2003; 229:570–574. [PubMed: 14595154]
45. Shah S, Watnick T, Atta MG. Not all renal cysts are created equal. *Lancet.* 2010; 376:1024. [PubMed: 20851261]
46. Kjaersgaard G, Madsen K, Marcussen N, et al. Tissue injury after lithium treatment in human and rat postnatal kidney involves glycogen synthase kinase-3beta-positive epithelium. *Am J Physiol Renal Physiol.* 2012; 302:F455–465. [PubMed: 22088436]
47. Christensen BM, Kim YH, Kwon TH, et al. Lithium treatment induces a marked proliferation of primarily principal cells in rat kidney inner medullary collecting duct. *Am J Physiol Renal Physiol.* 2006; 291:F39–48. [PubMed: 16434572]
48. Christensen BM, Marples D, Kim YH, et al. Changes in cellular composition of kidney collecting duct cells in rats with lithium-induced NDI. *Am J Physiol Cell Physiol.* 2004; 286:C952–964. [PubMed: 14613889]
49. Ravichandran K, Zafar I, Ozkok A, et al. An mTOR kinase inhibitor slows disease progression in a rat model of polycystic kidney disease. *Nephrol Dial Transplant.* 2014 [Epub ahead of print].
50. Bukanov NO, Moreno SE, Natoli TA, et al. CDK inhibitors R-roscovitine and S-CR8 effectively block renal and hepatic cystogenesis in an orthologous model of ADPKD. *Cell Cycle.* 2012; 11:4040–4046. [PubMed: 23032260]
51. Seeger-Nukpezah T, Proia DA, Egleston BL, et al. Inhibiting the HSP90 chaperone slows cyst growth in a mouse model of autosomal dominant polycystic kidney disease. *Proc Natl Acad Sci.* 2013; 110:12786–12791. [PubMed: 23858461]

52. Sabbatini M, Russo L, Cappellaio F, et al. Effects of combined administration of rapamycin, tolvaptan, and AEZ-131 on the progression of polycystic disease in PCK rats. *Am J Physiol Renal Physiol.* 2014; 306:F1243–1250. [PubMed: 24647711]
53. Hopp K, Hommerding CJ, Wang X, et al. Tolvaptan plus pasireotide shows enhanced efficacy in a PKD1 Model. *J Am Soc Nephrol.* 2014; 11:4257–73.
54. Harris PC, Torres VE. Polycystic kidney disease. *Annu Rev Med.* 2009; 60:321–337. [PubMed: 18947299]
55. Hopp K, Ward CJ, Hommerding CJ, et al. Functional polycystin-1 dosage governs autosomal dominant polycystic kidney disease severity. *J Clin Invest.* 2012; 122:4257–4273. [PubMed: 23064367]
56. Chang MY, Ong AC. New treatments for autosomal dominant polycystic kidney disease. *Br J Clin Pharmacol.* 2013; 76:524–535. [PubMed: 23594398]
57. Song X, Di Giovanni V, He N, et al. Systems biology of autosomal dominant polycystic kidney disease (ADPKD): computational identification of gene expression pathways and integrated regulatory networks. *Hum Mol Genet.* 2009; 18:2328–2343. [PubMed: 19346236]
58. Iglesias DM, Hueber PA, Chu L, et al. Canonical WNT signaling during kidney development. *Am J Physiol Renal Physiol.* 2007; 293:F494–500. [PubMed: 17494089]
59. Miller MM, Iglesias DM, Zhang Z, et al. T-cell factor/beta-catenin activity is suppressed in two different models of autosomal dominant polycystic kidney disease. *Kidney intl.* 2011; 80:146–153.
60. Schmidt-Ott KM, Masckauchan TN, Chen X, et al. beta-catenin/TCF/Lef controls a differentiation-associated transcriptional program in renal epithelial progenitors. *Development.* 2007; 134:3177–3190. [PubMed: 17693601]
61. Sugiyama N, Tsukiyama T, Yamaguchi TP, et al. The canonical Wnt signaling pathway is not involved in renal cyst development in the kidneys of inv mutant mice. *Kidney intl.* 2011; 79:957–965.
62. Hoeflich KP, Luo J, Rubie EA, et al. Requirement for glycogen synthase kinase-3beta in cell survival and NF-kappaB activation. *Nature.* 2000; 406:86–90. [PubMed: 10894547]
63. Ougolkov AV, Billadeau DD. Targeting GSK-3: a promising approach for cancer therapy? *Future Oncol.* 2006; 2:91–100. [PubMed: 16556076]
64. Sato N, Meijer L, Skaltsounis L, et al. Maintenance of pluripotency in human and mouse embryonic stem cells through activation of Wnt signaling by a pharmacological GSK-3-specific inhibitor. *Nat Med.* 2004; 10:55–63. [PubMed: 14702635]
65. Trowbridge JJ, Xenocostas A, Moon RT, et al. Glycogen synthase kinase-3 is an in vivo regulator of hematopoietic stem cell repopulation. *Nat Med.* 2006; 12:89–98. [PubMed: 16341242]
66. Kerkela R, Kockeritz L, Macaulay K, et al. Deletion of GSK-3beta in mice leads to hypertrophic cardiomyopathy secondary to cardiomyoblast hyperproliferation. *J Clin Invest.* 2008; 118:3609–3618. [PubMed: 18830417]
67. Shakoory A, Mai W, Miyashita K, et al. Inhibition of GSK-3 beta activity attenuates proliferation of human colon cancer cells in rodents. *Cancer Sci.* 2007; 98:1388–1393. [PubMed: 17640304]
68. Ougolkov AV, Fernandez-Zapico ME, Savoy DN, et al. Glycogen synthase kinase-3beta participates in nuclear factor kappaB-mediated gene transcription and cell survival in pancreatic cancer cells. *Cancer Res.* 2005; 65:2076–2081. [PubMed: 15781615]
69. Kunnimalaiyaan M, Vaccaro AM, Ndiaye MA, et al. Inactivation of glycogen synthase kinase-3beta, a downstream target of the raf-1 pathway, is associated with growth suppression in medullary thyroid cancer cells. *Mol Cancer Ther.* 2007; 6:1151–1158. [PubMed: 17363508]
70. Kim HM, Kim CS, Lee JH, et al. CG0009, a novel glycogen synthase kinase 3 inhibitor, induces cell death through cyclin D1 depletion in breast cancer cells. *PloS one.* 2013; 8:e60383. [PubMed: 23565238]
71. Cao Q, Lu X, Feng YJ. Glycogen synthase kinase-3beta positively regulates the proliferation of human ovarian cancer cells. *Cell Res.* 2006; 16:671–677. [PubMed: 16788573]
72. Bilim V, Ougolkov A, Yuuki K, et al. Glycogen synthase kinase-3: a new therapeutic target in renal cell carcinoma. *Br J Cancer.* 2009; 101:2005–2014. [PubMed: 19920820]

73. Omori S, Hida M, Fujita H, et al. Extracellular signal-regulated kinase inhibition slows disease progression in mice with polycystic kidney disease. *J Am Soc Nephrol.* 2006; 17:1604–1614. [PubMed: 16641154]

Author Manuscript

Author Manuscript

Author Manuscript

Author Manuscript

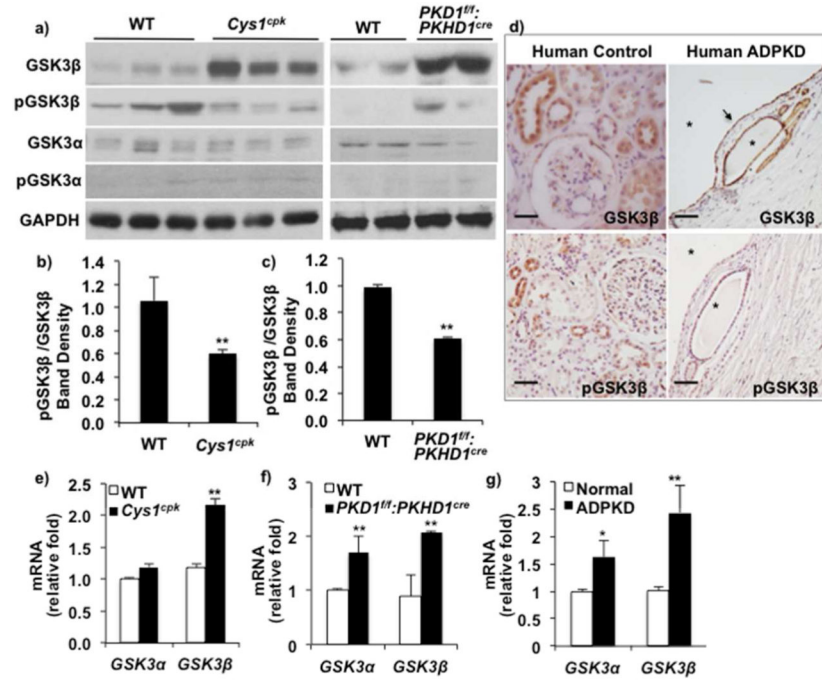


Fig 1. Renal GSK3β expression is upregulated in PKD

(a) Western blot analysis shows increased renal GSK3β in *Cys1^{cpk}* (P14) and *PKD1^{ff}:PKHD1^{cre}* mice (P21) compared to WT littermates. (b) Ratio of inactive pGSK3β-Serine 9 to total GSK3β is decreased in *Cys1^{cpk}* and (c) *PKD1^{ff}:PKHD1^{cre}* mice. (d) Immunostaining shows high GSK3β levels (arrow) and low pGSK3β levels in cyst-lining epithelium in human ADPKD kidney. (Star indicates cyst, scale bar=25μm) (e) qRT-PCR shows increased *GSK3β* mRNA relative to *18S* mRNA in *Cys1^{cpk}* mice, (f) *PKD1^{ff}:PKHD1^{cre}* mice and (g) human ADPKD kidney. *P<0.05, **P<0.01 compared to WT mice, n=6 mice/group.

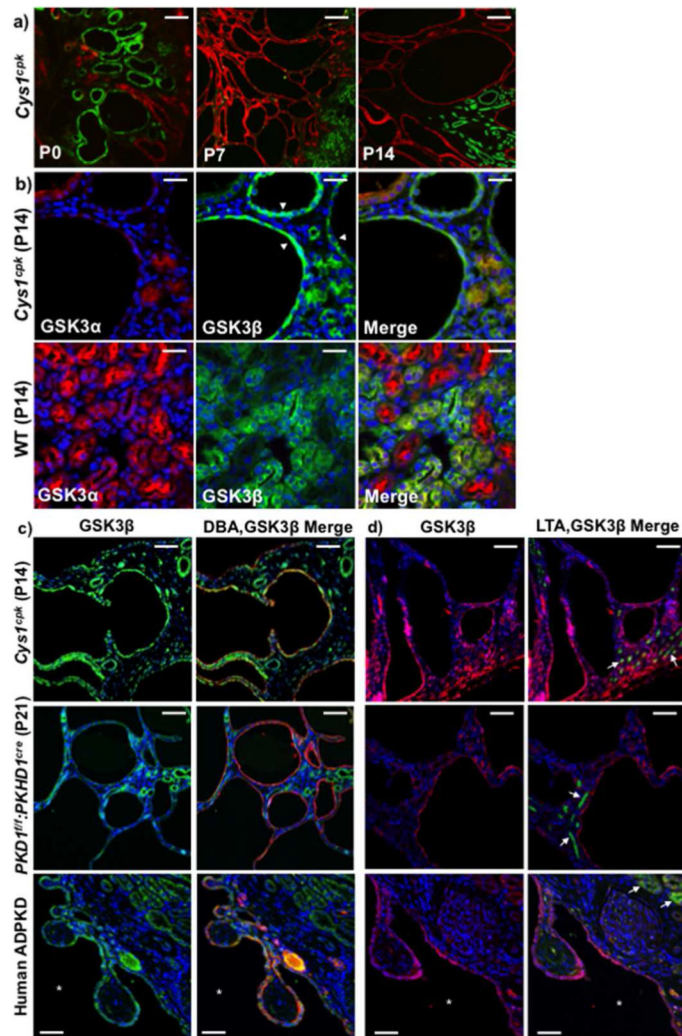


Fig 2. GSK3 β is expressed in cyst lining epithelium

(a) *Cys1^{cpk}* kidneys show LTA (green) staining cysts at P0 and DBA (red) staining cysts at P7 and P14. Scale bar=50 μ m. (b) At P14, *Cys1^{cpk}* kidneys show GSK3 β (green) staining in cyst-lining epithelium (white arrow heads) and GSK3 α (red) in non-cystic tubules. In wild type mice show ubiquitous staining for GSK3 α and GSK3 β in renal tubules. Scale bar=25 μ m (c) Immunofluorescence staining for GSK3 β (green) and DBA (red, representing collecting ducts) and (d) GSK3 β (red) and LTA (green, representing proximal tubules-white arrows) in *Cys1^{cpk}*, *PKD^{fl/fl}:PKHD1^{cre}* mice and human PKD kidneys. DAPI (blue) staining indicates nucleus in all figures. Scale bar=50 μ m.

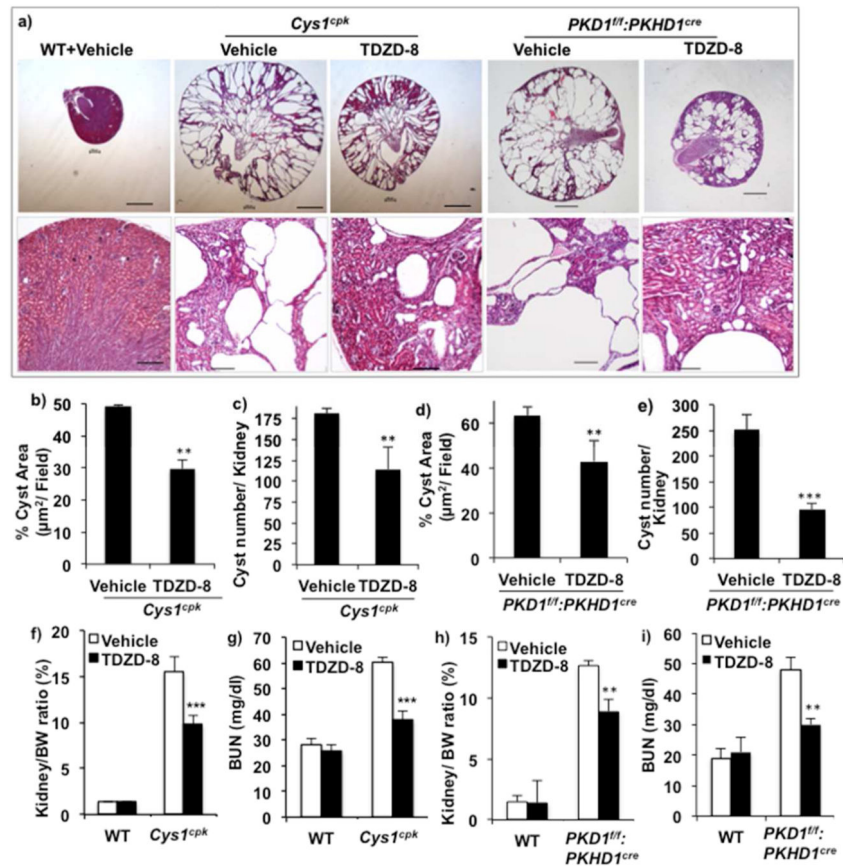
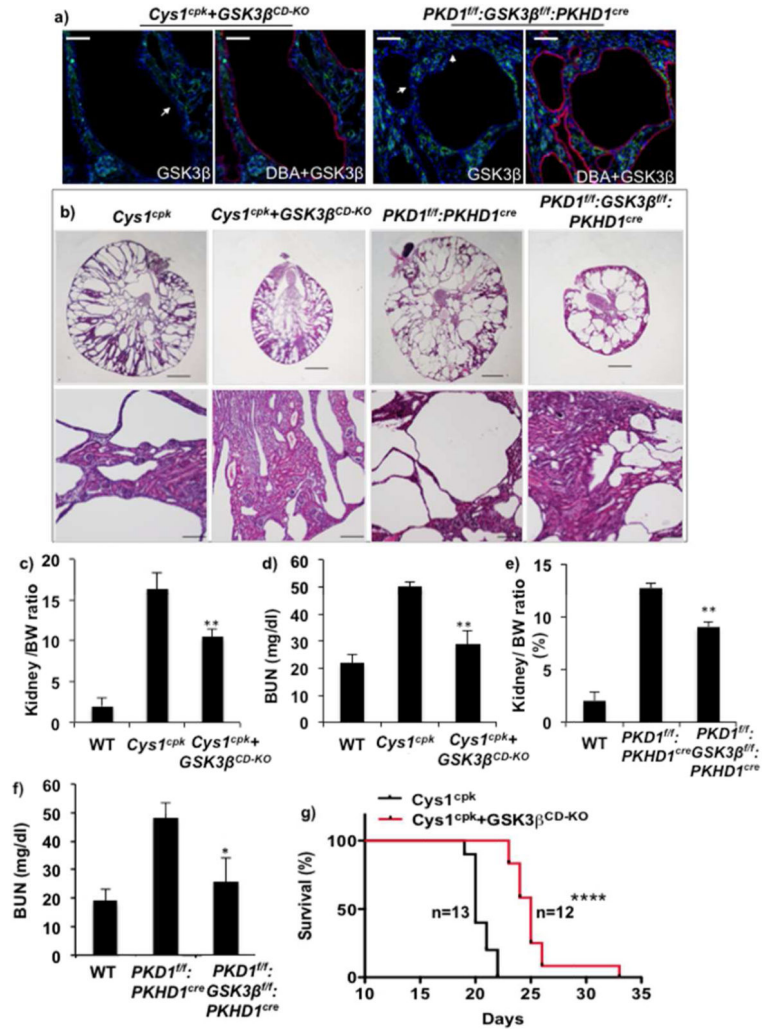


Fig 3. Systemic inhibition of GSK3 slows cyst expansion and progression of PKD in *Cys1^{cpk}* and *PKD1^{ff}:PKHD1^{cre}* mice. *Cys1^{cpk}* mice, *PKD1^{ff}:PKHD1^{cre}* mice and their WT littermates were treated with vehicle or TDZD-8. Analysis of P14 tissue in *Cys1^{cpk}* mice and P21 tissue in *PKD1^{ff}:PKHD1^{cre}* mice are shown. (a) TDZD-8 treated *Cys1^{cpk}* and *PKD1^{ff}:PKHD1^{cre}* mice had smaller kidneys with more intact parenchyma. Scale bar=1mm, Magnified images, Scale bar=100 μm (b) cyst area and (c) cyst number in *Cys1^{cpk}* mice (n=6/group). (d) cyst area and (e) cyst number in *PKD1^{ff}:PKHD1^{cre}* mice (n=6/group). (f) Kidney to body weight ratio and (g) blood urea nitrogen levels in *Cys1^{cpk}* mice (n=10/ group). (h) Kidney to body weight ratio and (i) blood urea nitrogen levels in *PKD1^{ff}:PKHD1^{cre}* mice (n=10/ group). **P<0.01, ***P<0.001, compared to vehicle treated mice.

**Fig 4.**

Renal collecting duct specific *GSK3 β* gene knockout reduces PKD in *Cys1^{cpk}* and *PKD1^{ff}:PKHD1^{cre}* mice. (a) *Cys1^{cpk}+GSK3^{CD-KO}* and *PKD1^{ff}:GSK3^β^{ff}:PKHD1^{cre}* mice lack GSK3 β (green) in DBA (red) staining collecting duct cells (white arrows). DAPI (blue) staining indicates nucleus. Scale bar=50 μ m (b) *Cys1^{cpk}+GSK3^{CD-KO}* and *PKD1^{ff}:GSK3^β^{ff}:PKHD1^{cre}* have smaller kidneys with more intact parenchyma. Scale bar=1mm, Magnified images, Scale bar=100 μ m (c) Kidney to body weight ratio and (d) blood urea nitrogen levels in *Cys1^{cpk}* mice (n=8/ group). (e) Kidney to body weight ratio and (f) blood urea nitrogen levels in *PKD1^{ff}:PKHD1^{cre}* mice (n=8/ group). (g) Survival curve shows median survival to be 25 days for *Cys1^{cpk}+GSK3^{CD-KO}* mice and 20 days for *Cys1^{cpk}* mice. *P<0.05, **P<0.01, ****P<0.0001, compared to *Cys1^{cpk}* or *PKD1^{ff}:PKHD1^{cre}* mice.

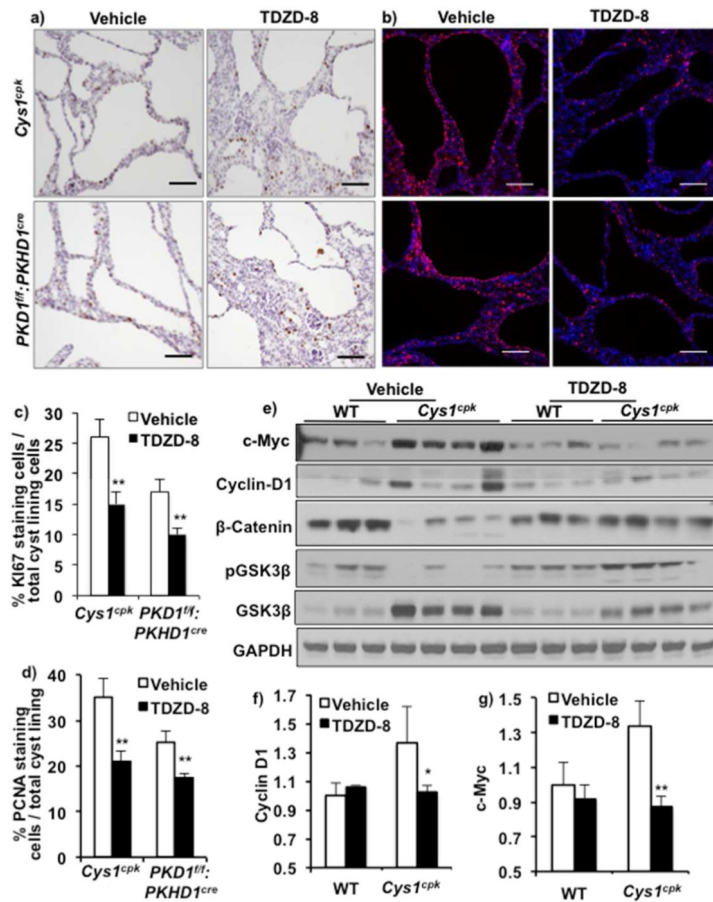
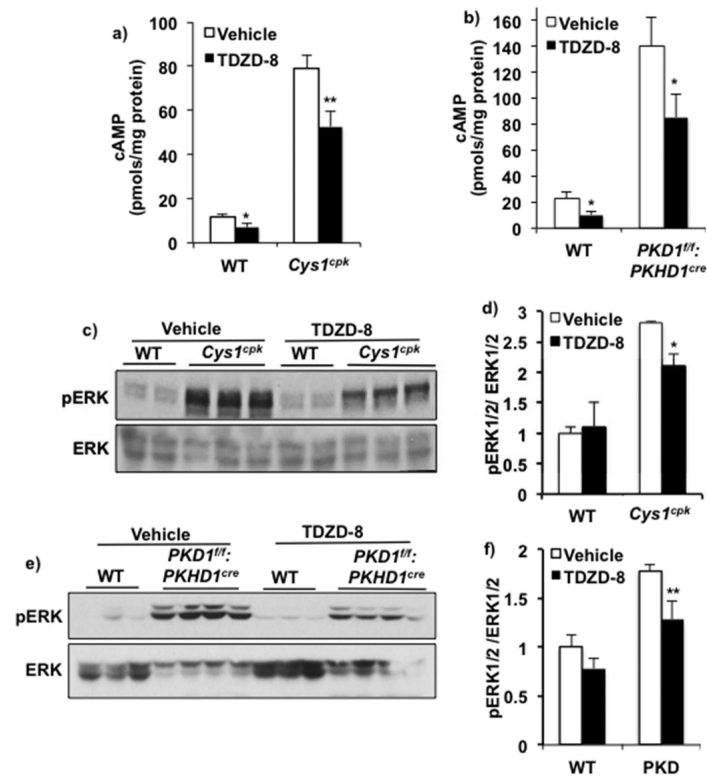


Fig 5. GSK3 inhibition reduced cell proliferation. (a) Cell proliferation measured by KI67 (brown) or (b) PCNA (pink) staining shows less proliferating cells in the cyst-lining epithelium of TDZD-8 treated *Cys1^{cpk}* (P14) and *PKD1^{ff}:PKHD1^{cre}* (P21) mice. DAPI (blue) staining indicates nucleus. (Scale bar=50μm). (c) Quantification of cyst-lining cells that stain for KI67 or (d) PCNA (n=6 mice/group). Data expressed as % dividing cells / total cyst lining cells. (e) Western blot analysis shows increase in c-Myc and Cyclin-D1 levels in *Cys1^{cpk}* compared to WT. TDZD-8 treatment reduces c-Myc and Cyclin-D1 in *Cys1^{cpk}* kidneys. (f) relative band density measurement for c-Myc and (g) Cyclin D1. *P<0.05, **P<0.01.

**Fig 6.**

GSK3 inhibition reduced renal cAMP. TDZD-8 treatment reduced renal cAMP concentration in (a) *Cys1^{cpk}* and (b) *PKD1^{ff}:PKHD1^{cre}* mice compared to vehicle treated mice. n=7 mouse kidneys/group. TDZD-8 treatment also reduced pERK to ERK ratio in (c,d) *Cys1^{cpk}* and (e,f) *PKD1^{ff}:PKHD1^{cre}* mice compared to vehicle treated mice. * $P < 0.05$, ** $P < 0.01$, TDZD-8 vs Vehicle treated.